Truncation mutants define and locate cytoplasmic barriers to lateral mobility of membrane glycoproteins

MICHAEL EDIDIN*†, MARTHA C. ZÚÑIGA‡, AND MICHAEL P. SHEETZ§

*Department of Biology, The Johns Hopkins University, Baltimore, MD 21218; ‡Department of Biology, University of California, Santa Cruz, CA 95064; and §Department of Cell Biology, Duke University Medical Center, Durham, NC 27710

ABSTRACT   The lateral mobility of cell membrane glycoproteins is often restricted by dynamic barriers. These barriers have been detected by measurements of fluorescence photobleaching and recovery (FPR) and barrier-free path (BFP). To define the location and properties of the barriers, we compared the lateral mobility, measured by FPR and BFP, of wild-type class I major histocompatibility complex (MHC) membrane glycoproteins with the lateral mobility of mutant class I MHC glycoproteins truncated in their cytoplasmic domains. Mutants with 0 or 4 residues in the cytoplasmic domain were as mobile as lipid-anchored class I MHC molecules, molecules whose lateral mobility is relatively unrestricted by barriers. In contrast, mobility of class I MHC molecules with 7-residue cytoplasmic domains was as restricted as mobility of class I molecules with full-length, 31-residue cytoplasmic domains. Though some of the difference between the mobilities of mutants with 4- or 0-residue domains and the other class I molecules may be due to differences in the net charge of the cytoplasmic domain, FPR measurements of the mobility of molecules with 7-residue domains show that length of the cytoplasmic domain has an important influence on the lateral mobility. Model calculations suggest that the barriers to lateral mobility are 2–3 nm below the membrane bilayer.

Barriers to the lateral mobility of plasma membrane proteins are found in many kinds of cells (1). These barriers were first suggested by fluorescence photobleaching and recovery (FPR) measurements (2–6). They were directly demonstrated by using a laser optical trap to drag membrane proteins, labeled by 40-nm gold beads, across the cell surface and measuring the barrier-free path (BFP) of these labeled proteins (7). Both FPR and BFP measurements showed that the barriers were dynamic. The extent of fluorescence recovery was higher and the BFPs were longer at 37°C than at 23°C. BFP and FPR estimates of the average distance between barriers were in good agreement, about 1 μm at 23°C. Experiments on the random walks of molecules labeled with gold beads also detected barriers to lateral diffusion on this scale (8–10).

FPR measurements did not detect barriers to the lateral movement of lipid-anchored membrane proteins, and the BFP of such proteins was ≈3 times that of homologous transmembrane proteins (7). This strongly suggested that the barriers to lateral mobility are in the cell cytoplasm. However, we could not rule out the possibility that the barriers were located in the membrane bilayer itself and could not establish the depth of the barriers beneath the membrane bilayer.

To distinguish between barriers located in the cell cytoplasm and barriers in the bilayer itself, we compared the BFPs of gold-labeled transmembrane proteins whose cytoplasmic domains were truncated to different extents. We find that the cytoplasmic domain, and not the presence of a transmembrane peptide, determines the BFP of these proteins. Unexpected differences between the behavior of the truncated proteins in the laser optical trap and in FPR experiments suggest that the interaction of a membrane protein with the cytoplasmic barriers depends upon the size of the protein's cytoplasmic domain and, perhaps, upon charged sequences which affect the domain's affinity for proteins of the cytoplasm. The data also allow us to estimate the distance from the cytoplasmic barriers to the inner surface of the plasma membrane.

MATERIALS AND METHODS

Cell Lines. HEPA-OVA mouse hepatoma cells express H-2D^b but not H-2K^b mouse class I major histocompatibility complex (MHC) molecules. HEPA-OVA-derived cell lines expressing the lipid-anchored class I MHC molecule Qa2 have been described (11). HEPA-OVA lines expressing mutant H-2L^d molecules truncated in their cytoplasmic domains were created by transfecting HEPA-OVA cells in suspension with calcium phosphate precipitates of the genomic clones of DNAs for BAL 911, C48, and 2.2.1 (see Fig. 1), together with neo, a gene for neomycin resistance. Six days after transfection, neomycin analogue G418 (600 μg/ml) was added to the culture medium [Dulbecco's modified Eagle's medium (DMEM) plus 10% fetal bovine serum]. After 2 weeks, surviving cells were checked for expression of H-2L^d by labeling with monoclonal antibody (mAb) 30.5.7 (12) and fluorescein-labeled goat anti-mouse Ig second antibody. The labeled cells gave two peaks by flow cytometry. One of these corresponded to the brightness of untransfected HEPA-OVA cells or of HEPA-OVA cells transfected with only neo. The average fluorescence intensity of cells in the second peak was 4–6 times that of the untransfected cells. Cells in this peak were selected by sorting and cultured. The cultured cells remained H-2L^d-positive, with only a small fraction of negative cells.

Labeling of Cells for FPR and BFP Measurements. For FPR we labeled cells with fluorescein-conjugated Fab fragments of mAb 30.5.7, specific for H-2L^d (12), and mAb 20.8.4, specific for Qa2 (13). Details of the preparation of the Fab fragments, of their conjugation with fluorescein isothiocyanate, and of cell labeling have been given elsewhere (6). Gold beads for BFP measurements were coated with intact mAb, as described (7). The antibody-coated beads bound specifically. Their binding was blocked by an excess of the appropriate free mAb.

In some FPR experiments, cells were labeled with plastic beads coated with fluorescein-conjugated Fab or IgG 30.5.7. To prepare these beads, 200 μl of a 2.5% suspension of 50-nm

Biophysics: Edidin *et al.*

Proc. Natl. Acad. Sci. USA 91 (1994)   3379

carboxylate latex beads (Polyscience) was mixed with 200 μl of fluorescein-conjugated IgG 30.5.7 (1.3 mg/ml) in phosphate-buffered saline at pH 7.3. The mixture was kept on ice for 30 min. Then 200 μl of fetal bovine serum was added and the suspension was centrifuged for 10 min in the right-angle head of a Beckman microcentrifuge. The yellow/orange pellet was washed twice with Hepes-buffered Hanks' balanced salt solution and resuspended in 200 μl of this solution by sonication in a bath sonicator. To determine the number of antibodies bound, a sample of beads suspended in DMEM was dissolved in 1 M NaOH and the OD_{490} was measured against a blank of DMEM. Knowing the fluorescein/protein ratio of the IgG used for coating, and taking the molar extinction coefficient of fluorescein as 80,000 $M^{-1}\cdot cm^{-1}$, we estimated that on average 40 IgG molecules were bound per bead in one batch of beads, and 30 molecules per bead in a second batch.

Measurement of BFP with Laser Optical Trap. An antibody-coated 40-nm gold bead, visualized by differential interference contrast optics, was trapped in a three-dimensional laser optical trap and dragged across the cell surface by translating a piezoelectric stage (Wye Creek Instruments, Frederick, MD) at ≈1 μm/s. The sequence of trapping, dragging, and escape from the trap was recorded on video tape. The BFP of trapped particles, the distance that they were dragged before meeting an obstacle and escaping the trap, could be measured from the video images by using stationary particles as reference points. Other details of our experiments were similar to those previously described (7), except that the optical trap used a Spectra–Physics ND:YLF solid-state laser

producing 1–3 W of 1040-nm light. The beam power at the trap was 50 mW.

FPR Measurements. Our FPR instrument and the way in which barriers to lateral mobility are inferred from FPR recoveries measured using different laser spot radii have been described at length (6).

Labeling of Cells with Fluorescent Plastic Beads. HEPA-OVA cells adherent to glass coverslips were labeled by incubation on ice with beads suspended in DMEM. After 30 min the beads were removed and the cells were washed three times with cold Hanks' balanced salt solution. Labeled cells were faintly stained at the surface and had little or no internal fluorescence. Aggregates of beads were also present, adherent to cells and to the coverslip. These were very much brighter than the ring stain and so could be avoided when FPR measurements were made.

RESULTS AND DISCUSSION

For our experiments on truncated membrane proteins we used mutants of the mouse class I MHC molecule H-2L^d. The cytoplasmic domains of three mutants and of the wild-type H-2D^b are diagramed in Fig. 1. The cytoplasmic domain of H-2D^b contains 31 amino acids and is identical to the full-length cytoplasmic domain of H-2L^d. The cytoplasmic domain of truncation mutant BAL 911 consists of 7 amino acids, the 6 membrane-proximal residues, KRRRNT, and the carboxyl-terminal A. The cytoplasmic domain of mutant C48 consists of 4 amino acids, KRSE (14). Thus it is not only shorter than the wild-type domain; it also lacks two of the positively-charged residues usually found at these positions
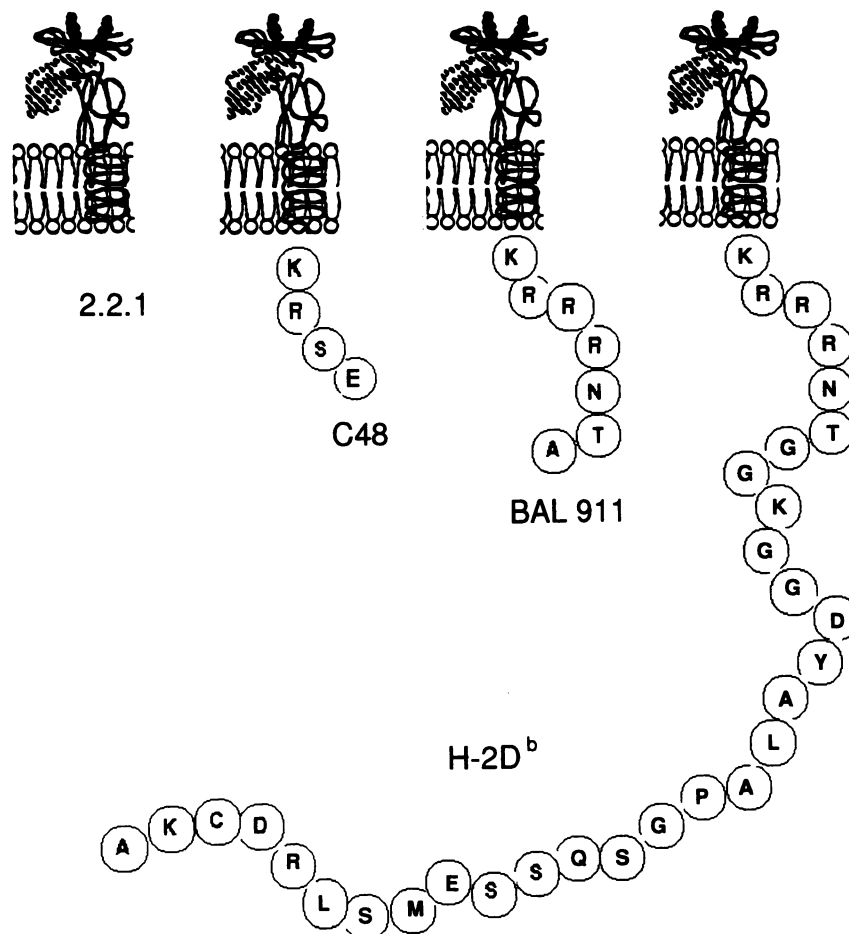

FIG. 1. Cytoplasmic domain sequences of H-2L^d mutants 2.2.1 (CT0), C48 (CT4), and BAL 911 (CT7), together with the sequence of the full-length cytoplasmic domain shared by H-2L^d and H-2D^b (CT31).

Table 1. BFPs of class I MHC molecules

Molecule	BFP, μm (mean ± SEM)	No. of measurements
CT31	1.2 ± 0.2	24
Qa2	2.1 ± 0.5	21
CT0	1.7 ± 0.2	38
CT4	2.0 ± 0.5	38
CT7	1.1 ± 0.2	58

in the wild-type and 7-residue cytoplasmic domains. Mutant 2.2.1 has no cytoplasmic domain at all (15). Throughout we refer to the wild-type class I MHC molecule as CT31 and to the mutants as CT7 (BAL 911), CT4 (C48), and CT0 (2.2.1). HEPA-OVA cell lines expressing each of the three mutant H-2L^d molecules were established as detailed in *Materials and Methods*. The HEPA-OVA line expressing the lipid-anchored class I MHC molecule Qa2 has been described (11).

BFPs of antibody-coated 40-nm gold beads bound to class I molecules were determined by using a three-dimensional laser optical trap. The average BFPs measured at room temperature, $\approx$23°C, are shown in Table 1. BFP for CT7 was 1.1 ± 0.2 μm, significantly lower than BFP for molecules with shorter cytoplasmic domains, CT4 and CT0, and close to the average BFP of a limited number of measurements of wild-type CT31 molecules, 1.2 ± 0.2 μm. BFPs of mutants CT4 and CT0 were similar to that Qa2, a lipid-anchored MHC molecule. The distributions of BFPs for the three mutants and Qa2 are shown in Fig. 2. It can be seen that >50% of the BFPs of CT7 molecules were in the range 0–0.5 μm. In contrast, <40% of the BFPs of CT4, CT0, and Qa2 were in the range 0–0.5 μm.

FPR measurements determine the diffusion coefficient, D, and the mobile fraction, R, of labeled membrane proteins in terms of recovery of fluorescence in a small area, a, bleached in an otherwise uniformly labeled cell surface (16–18). If there are no barriers to lateral diffusion of membrane proteins, then R is independent of a. If there are barriers to lateral diffusion, then R decreases with increasing a (5, 6). D also changes, often by an order of magnitude, with increasing a, apparently because measurements at small a do not detect contributions to recovery from molecules with very large D, whereas measurements at large a do not detect contributions to recovery from molecules with very small D (6).

R and D values for wild-type H-2D^b and for the mutant class I MHC molecules are in Table 2. Consistent with the BFP results, R of CT31 decreased as a increased, whereas R of mutant CT4 did not change even when a was increased to 28 μm^2. The R value of CT0 was also unaffected by an increase in a. For all these molecules, D increased with increasing a, as observed (and discussed) before (5, 6). On the basis of BFP measurements, we expected that R of mutant CT7 would decrease with increased a in the same way as R of the wild-type class I MHC molecule. However, R was the
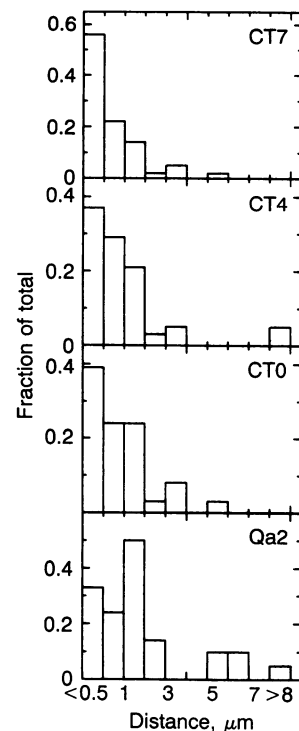

FIG. 2. Distribution of BFP for truncated H-2L^d molecules CT7, CT4, and CT0 and for the lipid-anchored class I MHC molecule Qa2, all expressed in HEPA-OVA cells. H-2L^d molecules were labeled by 40-nm gold beads coated with mAb 30.5.7. This mAb is specific for H-2L^d and does not bind the endogenous H-2D^b of HEPA-OVA cells. Qa2 molecules were labeled by beads coated with mAb 20.8.4.

same for $a = 1.1$ μm^2 as for $a = 4.5$ μm^2. R decreased, to 22 ± 4%, only for $a = 28$ μm^2.

The FPR results for CT31, CT4, and CT0 are consistent with the BFPs measured for these molecules. The results for CT0, a molecule with a transmembrane domain but no cytoplasmic domain, rule out the possibility that the barriers to lateral mobility that we described earlier (7) were in the membrane bilayer rather than in the cytoplasm. The FPR results for CT4 are also consistent with the BFPs. Both sets of measurements imply that the short cytoplasmic domain of CT4 does not meet barriers to lateral mobility as frequently as the cytoplasmic domain of wild-type, CT31, class I MHC molecules.

The FPR results for CT7 are not consistent with the BFP for this molecule. While the BFP of CT7 molecules is like that of wild-type MHC I molecules, the FPR data of Table 2 show that single CT7 molecules meet barriers less often than do wild-type class I MHC molecules, but more often than CT4 molecules. R of CT7 did not change when a was increased from 1.1 to 4.5 μm^2, but it decreased for $a = 28$ μm^2. The net

Table 2. Mobile fraction, R, and diffusion coefficient, D, of wild-type and truncated class I MHC molecules

a, μm^2	CT31			CT0			CT4			CT7		
	R	D	n	R	D	n	R	D	n	R	D	n
				Molecules labeled with fluoresceinated Fab fragments								
1.1	43 ± 3	13	15	42 ± 3	3	20	40 ± 2	17	29	39 ± 2	5	46
4.5	**33 ± 4**	74	13	45 ± 4	16	18	38 ± 2	50	19	40 ± 2	19	50
28	ND	ND	—	ND	ND	—	38 ± 3	220	22	**22 ± 4**	60	9
				Molecules labeled with fluorescein-IgG-coated 50-nm plastic beads								
1.1							37 ± 3	8	29	38 ± 3	9	40
4.5							41 ± 3	70	22	**27 ± 3**	50	26

R is given as percent recovery (mean ± SEM); D is units of 10^{-10} cm^2·s^{-1}; n is the number of measurements. Values of R in boldface type are significantly smaller than other R values in the same column. In a two-sided Student's t test for CT31, $0.01 < P < 0.05$. For CT7, $P < 0.01$ for both comparisons.

charge of the CT7 cytoplasmic sequence is the same as that of the equivalent sequence in wild-type, CT31 molecules. Hence, the FPR data indicate that the length of the CT7 domain, rather than its charge, is important in avoiding or passing cytoplasmic barriers to lateral diffusion.

Labels for FPR are monovalent or divalent; hence, they report mainly the lateral diffusion of single H-2L^d molecules. In contrast, the antibody-coated beads used for BFP measurements are multivalent and bind to many H-2L^d molecules at once. The actual valence of such beads has not been measured, but it is known that the lateral diffusion coefficients reported by antibody-coated beads depend upon the amount of antibody used to coat them (19). With this in mind, we labeled mutant CT7 and CT4 molecules with 50-nm carboxylate latex beads coated with an average of 30–40 fluorescent 30.5.7 IgG molecules per bead. D values of CT4 labeled with these beads was about the same as D values for mutants labeled with fluorescent Fab fragments (compare values at the top and bottom of the column for C48 of Table 2). As before, R did not change when a was increased. D values of CT7 labeled with fluoresceinated Ig-coated beads or with fluoresceinated Fab fragments were also similar. R values of bead-labeled molecules did change with a.

The experiments just described indicate that the lateral diffusion of small aggregates of CT7 is more restricted by cytoplasmic structures than is the lateral diffusion of single CT7 molecules. This may be because the gaps in the cytoplasmic barriers are on average large enough to pass single molecules of CT7 but not large enough to pass clusters of these molecules. It also may be due to the enhanced binding of clustered CT7 to low-affinity binding sites in the cytoplasm. If the clustered CT7 molecules bound soluble molecules of the cytoplasm this could decrease BFP, by increasing the volume of the units passing through gaps in dynamic barriers. If clustered CT7 molecules bound transiently to the cytoskeleton, this would also reduce their measured BFP. Determination of the size of CT7 aggregates may allow a choice between these possibilities.

Although it is difficult to move from the mechanical definition of the barriers to a molecular definition, two obvious mechanisms can be considered: a barrier may bind diffusing proteins or it may act as a mechanical or other form of repulsive barrier to their passage. In the case of binding interactions, the cytoplasmic tail of an H-2L^d molecule could bind proteins of the barrier through electrostatic or stereospecific interactions. However, this is not the case for CT7. Even though it has the same cluster of basic amino acids as the wild-type class I MHC molecule, this mutant does not behave like a wild-type molecule in FPR measurements. R of CT7 is much less dependent on a than is R of wild-type, CT31 molecules, implying that the lateral mobility of single CT7 molecules is less restricted by barriers than is the lateral mobility of CT31. This is consistent with a mechanical model for the barriers but not consistent with a binding/electrostatics model. On the other hand, part of the population of bead-labeled molecules and a fraction of Fab-labeled molecules are immobile, implying that they are tethered to some elements of the cytoskeleton. Hence, the behavior of aggregated CT7 labeled by gold or plastic beads and the increased BFP and FPR behavior of CT4 can be explained by a binding interaction model, or by a mechanical or pure barrier model, or by some combination of the two.

In most instances we observed that beads resumed rapid diffusion after encountering barriers and being pulled from the trap. Thus for mobile molecules the interaction with the barrier exerts a large mechanical force, but only for the time of physical contact. In these cases the barriers appear to be primarily repulsive in nature and not trapping. The rapid resumption of diffusion after leaving the trap also means that trapped molecules are not tethered to an elastic cytoskeleton,

since tethered molecules snap away from their point of exit from the trap rather than resume rapid diffusion (20).

Mechanical barriers to lateral mobility could be located at the inner surface of the bilayer itself, interacting directly with phospholipids (see refs. 21 and 22), or in the cytoplasm some distance below the bilayer (for models of the relationship between membrane or cytoskeleton and the inner surface of the plasma membrane, see refs. 23–25). We can probably rule out a barrier bound tightly to lipid head groups, because even a single 7-residue tail containing 4 basic residues would resist being dragged into the lipid phase of the bilayer and hence could not shorten sufficiently to clear the barriers. The location of barriers at some distance from the inner surface of the bilayer can be estimated by using the distributions of end-to-end distances of water-soluble 4- to 9-residue oligopeptides that were measured by Haas *et al.* (26). Though the synthetic peptides used did not contain the sequences of the cytoplasmic domains of class I MHC molecules and though the cluster of basic residues might interact with bilayer lipids to reduce chain extensions, the results of ref. 26 allow a first approximation to the distances from the bilayer that are probed by CT4 and CT7. Fig. 3 shows the distribution of distances below the membrane bilayer for the ends of the 4-residue tail of CT4 (*Upper*) and the 7-residue tail of CT7 (*Lower*) calculated from ref. 26. Seven-residue tails could stably extend >2 nm into the cytoplasm, whereas 4-residue tails could not. Depending upon the structural rigidity of the tails, a barrier lying from 2 to 3 nm away from the lipid surface would offer sufficient resistance to pull a bead (attached to membrane glycoproteins) from the trap. This distance is consistent with the size of the cytoplasmic domains of many multispanning membrane proteins and the cytoskeletal components that often bind to them. Diffusion of these or other membrane proteins through the mesh of a cytoskeleton slightly separated from the lipid bilayer surface requires transient gaps in the mesh, effectively creating dynamic,
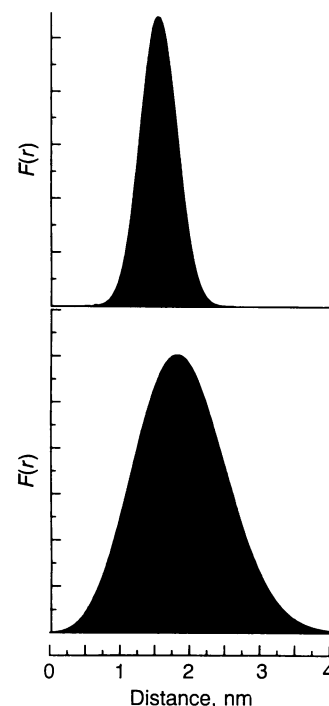

FIG. 3. Probability $F(r)$ of reaching a given depth below the bilayer for CT4, an H-2L^d molecule with a 4-residue cytoplasmic domain (*Upper*), and CT7, an H-2L^d molecule with a 7-residue cytoplasmic domain (*Lower*). The horizontal scale indicates distance from the inner surface of the membrane bilayer. Values were calculated from expression 1 of ref. 26.

protein-rich membrane domains of the order of 1 μm in size. These domains serve, together with other molecular restraints, including direct anchoring to the cytoskeleton and molecular clustering, to organize cell surface membrane architecture and function.

1. Edidin, M. (1992) *Trends Cell Biol.* **2**, 376–380.
2. Sheetz, M. P., Schindler, M. & Koppel, D. E. (1980) *Nature (London)* **285**, 510–512.
3. Golan, D. E. & Veatch, W. (1980) *Proc. Natl. Acad. Sci. USA* **77**, 2537–2541.
4. Shields, M., La Celle, P., Waugh, R. E., Scholz, M., Peters, R. & Passow, H. (1987) *Biochim. Biophys. Acta* **905**, 181–194.
5. Yechiel, E. & Edidin, M. (1987) *J. Cell Biol.* **105**, 755–760.
6. Edidin, M. & Stroynowski, I. (1990) *J. Cell Biol.* **112**, 1143–1150.
7. Edidin, M., Kuo, S. C. & Sheetz, M. P. (1991) *Science* **254**, 1379–1382.
8. Sheetz, M., Turney, S., Qian, H. & Elson, E. (1989) *Nature (London)* **340**, 284–288.
9. de Brabander, M., Nuydens, R., Ishihara, A., Holifield, B., Jacobson, K. & Geerts, H. (1991) *J. Cell Biol.* **112**, 114–124.
10. Kusumi, A., Sako, Y. & Yamamoto, M. (1993) *Biophys. J.* **65**, 2021–2040.
11. Stroynowski, I., Soloski, M., Low, M. G. & Hood, L. E. (1987) *Cell* **50**, 759–768.
12. Murre, C., Choi, E., Weis, J., Seidman, J., Ozato, K., Liu, L., Burakoff, S. & Reiss, C. (1984) *J. Exp. Med.* **160**, 167–178.
13. Ozato, K. & Sachs, D. (1980) *J. Immunol.* **125**, 2473–2477.
14. Zuniga, M., Malissen, B., McMillan, M., Brayton, P. R., Clark, S. S., Forman, J. & Hood, L. (1983) *Cell* **34**, 535–544.
15. Zuniga, M. C. & Hood, L. E. (1986) *J. Cell Biol.* **102**, 1–10.
16. Jovin, T. M. & Vaz, W. L. C. (1988) *Methods Enzymol.* **172**, 471–513.
17. Matko, J., Szollosi, J., Tron, L. & Damjanovich, S. (1988) *Q. Rev. Biophys.* **21**, 479–544.
18. Wolf, D. E. (1989) *Methods Cell Biol.* **30**, 271–306.
19. Lee, G. M., Zhang, F., Ishihara, A., McNeil, C. L. & Jacobson, K. A. (1993) *J. Cell Biol.* **120**, 25–35.
20. Schmidt, C. E., Horwitz, A. F., Lauffenburger, D. A. & Sheetz, M. P. (1993) *J. Cell Biol.* **123**, 977–991.
21. Devaux, P. F. (1991) *Biochemistry* **30**, 1163–1173.
22. Kinnunen, P. J. K. (1991) *Chem. Phys. Lipids* **57**, 375–399.
23. Bennett, V. (1990) *Physiol. Rev.* **70**, 1029–1065.
24. Luna, E. J. & Hitt, A. L. (1992) *Science* **258**, 955–964.
25. Stossel, T. P. (1993) *Science* **260**, 1086–1094.
26. Haas, E., Wilchek, M., Katchalski-Katzir, E. & Steinberg, I. Z. (1975) *Proc. Natl. Acad. Sci. USA* **72**, 1807–1811.